"Cristal Tachycardias": Origin of Right Atrial Tachycardias From the Crista Terminalis Identified by Intracardiac Echocardiography

JONATHAN M. KALMAN, MBBS, PhD, FACC,* JEFFREY E. OLGIN, MD,
MARTIN R. KARCH, MD, MOHAMED HAMDAN, MD, RANDALL J. LEE, MD, PhD, FACC,
MICHAEL D. LESH, MD, FACC

San Francisco, California

Objectives. We sought to use intracardiac echocardiography (ICE) to identify the anatomic origin of focal right atrial tachycardias and to define their relation with the crista terminalis (CT).

Background. Previous studies using ICE during mapping of atrial flutter and inappropriate sinus tachycardia have demonstrated an important relation between endocardial anatomy and electrophysiologic events. Recent studies have suggested that right atrial tachycardias may also have a characteristic anatomic distribution.

Methods. Twenty-three consecutive patients with 27 right atrial tachycardias were included in the study. ICE was used to facilitate activation mapping in relation to endocardial structures. A 20-pole catheter was positioned along the CT under ICE guidance. ICE was also used to assist in guiding detailed mapping with the ablation catheter in the right atrium.

Results. Of 27 focal right atrial tachycardias, 18 (67%, 95% confidence interval [CI] 46% to 83%) were on the CT (2 high medial, 8 high lateral, 6 mid and 2 low). ICE identified the location of the tip of the ablation catheter in immediate relation to the CT in all 18 cases. The 20-pole mapping catheter together with echocardiographic visualization of the CT provided a guide to the site of tachycardia origin along this structure. Radiofrequency ablation was successful in 26 (96%) of 27 (95% CI 81% to 100%) right atrial tachycardias.

Conclusions. This study demonstrates that approximately two thirds of focal right atrial tachycardias occurring in the absence of structural heart disease will arise along the CT. Recognition of this common distribution may potentially facilitate mapping and ablation of these tachycardias.

(J Am Coll Cardiol 1998;31:451–9)
©1998 by the American College of Cardiology

During radiofrequency ablation of atrial tachycardias, complex three-dimensional mapping within the body of the right and left atria is required, and various techniques have been proposed to facilitate such mapping (1–7). These have included methods such as use of two mapping catheters in leapfrog style, in an attempt to locate the earliest site of activation (1,3), or use of paced endocardial activation sequence mapping (2).

We (8) previously reported the use of intracardiac electrocardiography (ICE) for accurate localization of a mapping catheter and for guiding radiofrequency mapping and ablative procedures (9–11). These studies demonstrated the important relation between endocardial anatomy and electrophysiologic phenomena during both atrial flutter (10) and inappropriate

sinus tachycardia (12). Right atrial tachycardias were previously reported (2,3,13,14) to have a characteristic anatomic distribution, but this characterization relied on fluoroscopy and direct endocardial visualization was not performed.

In the current study we used ICE to test the hypothesis that there is a relation between atrial endocardial anatomy and the distribution of right atrial tachycardias. In particular, we hypothesized that the majority of right atrial tachycardias will be distributed along the long axis of the crista terminalis (CT).

Methods

Patient groups. *Inclusion criteria.* Patients were included in this study when a right atrial tachycardia was suspected on the basis of clinical and electrocardiographic (ECG) criteria. Patients with the syndrome of inappropriate sinus tachycardia and patients with reentrant atrial tachycardia complicating surgically repaired congenital heart disease were not included. All antiarrhythmic drugs were stopped at least 5 half-lives before study. No patient had been treated with amiodarone.

Definitions. Atrial tachycardia was diagnosed according to well accepted criteria (1,15). Fractionated electrograms were defined as a potential with multiple peaks and a duration of >40 ms, as previously described (16). Atrial tachycardias were considered to be arising from the CT when ICE (see later)

Abbreviations and Acronyms

AV   = atrioventricular
CI   = confidence interval
CS   = coronary sinus
CT   = crista terminalis
ECG = electrocardiogram, electrocardiographic
ICE = intracardiac echocardiography (echocardiographic)

---

revealed the characteristic fan-shaped artifact of the tip of the ablation catheter in contact with the CT at the site of successful ablation.

All data are presented as mean value ± SD and statistical analyses are by analysis of variance, *t* test or Fisher exact test where appropriate. Confidence intervals of proportions were calculated by using the exact method.

Intracardiac echocardiography. The intracardiac imaging system has been previously described (8,9). Briefly this consists of a 10-MHz rotating ultrasound transducer mounted at the tip of a 10F catheter (CVIS). The imaging catheter was introduced by way of a 10F sheath in the left femoral vein and positioned in the superior vena cava. The imaging catheter was then gradually withdrawn through the body of the right atrium to immediately below the junction of the right atrium with the inferior vena cava in order to first fully characterize the anatomic location and extent of the CT and other right atrial anatomic structures. Sequential views of the right atrium and the structures visualized by using this method are shown in Figure 1. ICE imaging was continuous throughout the study and all applications were recorded on super VHS videotape for subsequent review.

Catheters. A 7F, 20-pole custom-designed steerable catheter (Cordis-Webster) with 1-mm interelectrode distance and 3-mm interbipole distance, was then positioned under ICE guidance in the right atrium along the long axis of the CT. This catheter was inserted by way of a long vascular sheath to ensure stability and assist with its placement in close apposition to the CT. Fluoroscopy of the CT catheter in position is shown in Figure 2. The catheter position was standardized such that the second bipole lay at the junction of the superior vena cava with the right atrium as determined by ICE. An 8F, open lumen, decapolar catheter (Elecath) (2-mm interelectrode distance and 5-mm intraelectrode distance) was placed by way of the internal jugular vein into the coronary sinus (CS). Positioning of the proximal electrode pair at the CS os was confirmed with contrast injection viewed with fluoroscopy. The CS catheter was sutured into place. A standard quadripolar electrode catheter was positioned in the His bundle recording position.

An 8F roving catheter (EP Technologies) (5-mm electrode tip, other electrodes 2 mm with 2-mm interelectrode spacing) was used for activation mapping and radiofrequency ablation. During mapping with ICE guidance, the catheter tip was identified by its characteristic fan-shaped acoustic shadow (8). When early sites were defined either from the 20-pole catheter or on the mapping catheter, further mapping was performed in that region in an attempt to record an even earlier and fractionated electrogram (1). At these sites, radiofrequency energy was applied with temperature feedback control to a target of 70°C with a maximal-allowed power output of 50 W.

Electrogram recordings and measurements. Bipolar intracardiac electrograms filtered between 30 and 500 Hz were recorded and stored digitally on a Cardiolab system (Prucka Engineering) simultaneously with 12-lead surface ECGs. All measurements were performed on the Cardiolab system at a screen speed of 400 mm/s by using on-screen digital calipers.

To carefully measure activation time to initial onset of the P wave, the 12-lead ECG was carefully analyzed during a period of atrioventricular (AV) block. The relation between the P wave and activation at the ostium of the CS (chosen because of the stability of the catheter location) was then
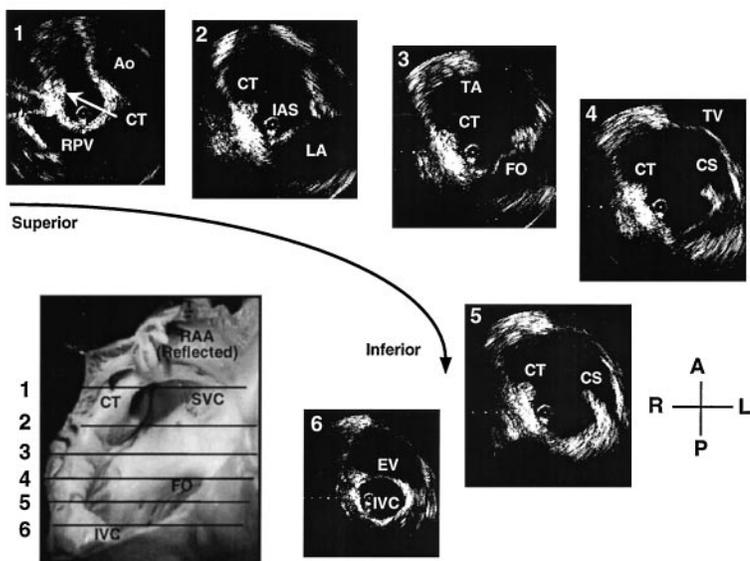

Figure 1. Schematic of the cut-open right atrium depicts the approximate level of the six sequential ICE sections through the right atrium. All sections show the prominent ridge of the CT at the junction of the posterior smooth-walled atrium with the anterior trabeculated atrium as it courses from its superior aspect at the superior vena cava–right atrial junction (seen on the schematic and on ICE section 1) to its inferior aspect, where it becomes continuous with the Eustachian valve (EV) anterior to the inferior vena cava (IVC) (seen on ICE section 6). Other structures seen include the right upper pulmonary vein (RPV) (section 1), the fossa ovalis (FO) (sections 2 and 3), the ostium of the coronary sinus (CS) (sections 4 and 5), the Eustachian valve (section 6), the IVC (section 6), the tricuspid annulus (TA) (sections 3 to 6) and the tricuspid valve (TV) (sections 3 to 5). A = anterior; Ao = aorta; IAS = interatrial septum; L = left; LA = left atrium; P = posterior; R = right; RAA = right atrial appendage.

Figure 2. Right (RAO) and left (LAO) anterior oblique fluoroscopic projections showing the mapping catheters in place and the location of the roving catheter on the superior and lateral CT. In the left anterior oblique projection the **short arrows** mark the right heart border, which is otherwise not clearly seen. The 20-pole catheter is deployed along the CT through a long vascular sheath. The tip of the roving catheter is in place on the superior and lateral CT at the site of ablation (Abl) of a tachycardia focus. Also shown are the His bundle electrogram (HBE) and CS catheters.
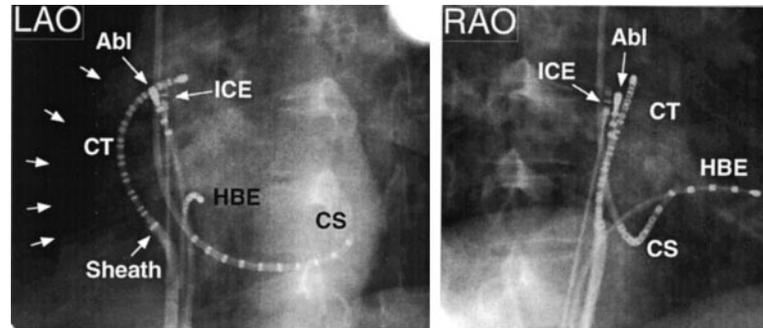
defined. During mapping, if the P wave onset could not always be clearly defined, activation time was measured to onset of activation at the ostium of the CS which occurred in a known fixed relation to P wave onset during tachycardia. Activation time was measured from onset of the first sharp electrogram component in the mapping catheter (17) to onset of the P wave.

Results

Patient characteristics. Included in the study were 27 patients in whom right atrial tachycardia was suspected on the basis of the 12-lead ECG configuration during tachycardia. In 23 patients, 27 focal tachycardias were localized to the right atrium. In the remaining four patients, atrial tachycardia was eventually localized to the right pulmonary vein. These patients are included in this report because the tachycardia P wave configuration was consistent with a possible right atrial focus. As a result, these patients underwent initial right atrial mapping with ICE guidance and a 20-pole catheter along the CT.

There were 10 male and 17 female patients with a mean age ± SD of 41.3 ± 14.2 years (range 11 to 66, 95% confidence interval [CI] 36 to 47). The mean symptom duration was 4.9 ± 2.9 years (95% CI 3.6 to 6.1), and the mean number of failed antiarrhythmic agents was 2.5 ± 1.7 (95% CI 1.8 to 3.3). Coexisting arrhythmias, treated at the same or a previous ablation session, occurred in seven patients and included typical AV node reentrant tachycardia (n = 3), atypical AV node reentrant tachycardia (n = 3) and right ventricular outflow tract tachycardia (n = 1). Two patients had depressed left ventricular systolic function (ejection fraction 45% and 20%, respectively) that in both cases was considered to represent a tachycardia-mediated cardiomyopathy. One patient had mitral valve prolapse; no other patients had structural heart disease.

Tachycardia characteristics. The mean tachycardia cycle length for 27 right atrial tachycardias was 378 ± 94 ms (range 246 to 545, 95% CI 342 to 413) and 362 ± 62 ms (range 271 to 410, 95% CI 301 to 423) for four pulmonary vein tachycardias.

Intracardiac echocardiographic observations. ICE allowed clear visualization of the CT in its full extent from superior, where it crosses anterior and medial to the superior vena cava at the superior vena cava–right atrial junction, to its inferior extent where it becomes continuous with the eustachian valve anterior to the inferior vena cava in all patients (Fig. 1). There was considerable variation in the physical characteristics of the CT. In all patients the ridge was prominent in its superior third. In 12 patients this continued as a prominent and clearly defined ridge in its middle third in the body of the right atrium. In seven patients, the CT remained detectable as a prominent ridge throughout its length. In the remaining patients, it became progressively less prominent as it progressed from superior to inferior such that in its inferior one third, a ridge was no longer discernible and the CT could be located only by determining the junction of the posterior smooth-walled atrium with the anterolateral trabeculated atrium. In addition, there was considerable variation in its anatomic course, which precluded attempts to accurately place the mapping catheter along the CT with fluoroscopy alone.

Anatomic distribution of tachycardias. *Right atrial tachycardias.* Of 27 focal right atrial tachycardias, 18 (67%, 95% CI 46% to 83%) were on the CT (2 high medial, 8 high lateral, 6 mid and 2 low). ICE identified the location of the tip of the ablation catheter in immediate relation to the CT in all cases (Fig. 3A and 4A). Seventeen of 23 patients (74%, 95% CI = 52% to 90%) with right atrial tachycardias had a tachycardia located along the CT.

Of the right atrial tachycardias not located on the CT, three were in the anterior trabeculated atrium. In one case, the successful site was near the tip of the appendage where the mapping catheter identified an early site with an activation time of −72 ms. At this site a mass (0.8 cm × 0.4 cm in maximal dimension) was clearly imaged with ICE and successful ablation was performed with the catheter abutting this mass. One tachycardia was ablated in the mid to superior region of the anterolateral atrium 1.5 cm anterior to the CT and one in the midanterolateral atrium.

Three right atrial tachycardias occurred on the tricuspid annulus between the 7:00 and 8:00 o'clock positions when viewing the tricuspid annulus in the left anterior oblique projection. All three of these patients had also previously undergone ablation of an atypical AV node tachycardia in the posteroseptal region (two at earlier ablative procedures and one at the same session).
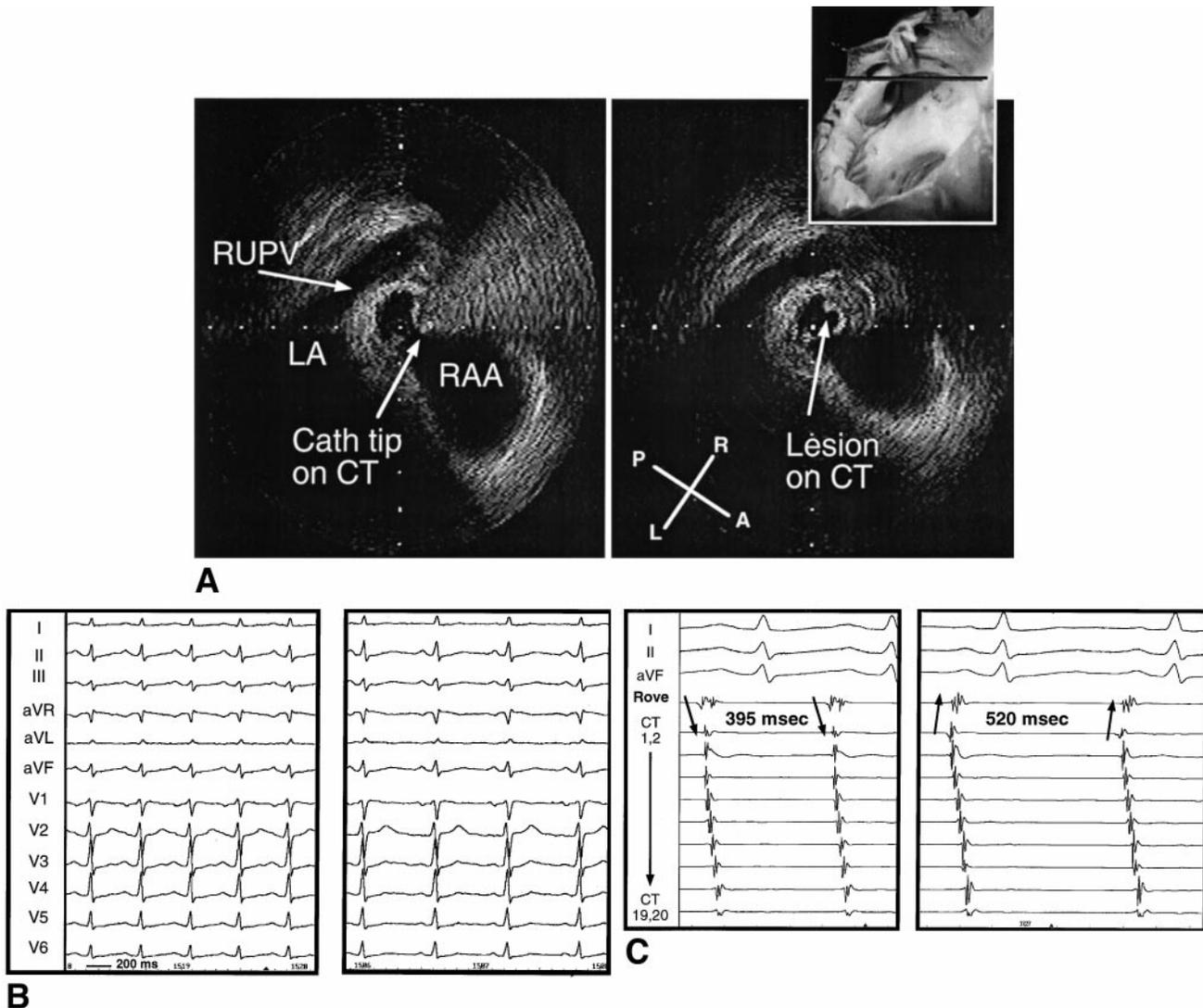
Figure 3. A, ICE view of the high CT showing the anatomic structures and the location of the ablation catheter (Cath) at the site of successful ablation **(left panel)** and the lesion after ablation **(right panel). B,** 12-lead ECG of sinus rhythm **(left panel)** and of atrial tachycardia arising from the superior CT **(right panel)** from the same patient. **C,** Endocardial activation pattern recorded on the 20-pole catheter (CT 1 to 20), during atrial tachycardia arising from the high CT **(left panel)** and during sinus rhythm **(right panel).** The roving catheter is located on the high lateral CT at the site of successful ablation. During atrial tachycardia, the activation sequence on the CT catheter is high to low and the roving catheter shows an early and fractionated signal. During sinus rhythm, the CT catheter activation sequence is again high to low, but the roving catheter at the same site now records a late signal, indicating that sinus activation is originating from a different focus. Activation along the CT appears to occur faster during atrial tachycardia than during sinus rhythm. RUPV = right upper pulmonary vein; other abbreviations as in Figure 1.

In addition, three atrial tachycardias were located on the smooth septal region of the right atrium, two adjacent to the mouth of the coronary sinus and one in the mid- to high posterior septum.

Left atrial tachycardias. There were four left-sided atrial tachycardias, two located at the orifice of the right upper pulmonary vein and two immediately between the orifice of the right upper and lower pulmonary veins. These pulmonary vein tachycardias had ECG criteria suggestive of a right atrial tachycardia and therefore underwent mapping as part of this study.

Surface ECG. Surface ECG P wave configuration according to tachycardia location is demonstrated in Table 1. Representative examples of the 12-lead ECG for tachycardias arising from the superior and mid-CT are shown in Figures 3B and 4B, respectively. In general, superior sites were associated with an upright inferior P wave (high CT, right upper pulmonary vein), and inferior sites with an inverted inferior P wave (CS os, low CT and inferior tricuspid annulus). There was considerable overlap of P wave configuration between superior right atrial sites and sites in the right pulmonary veins. Only 4 of 27 (15%, 95% CI 4% to 34%) right atrial tachycardias had an inverted P wave in lead aVL, and all of these were located on the
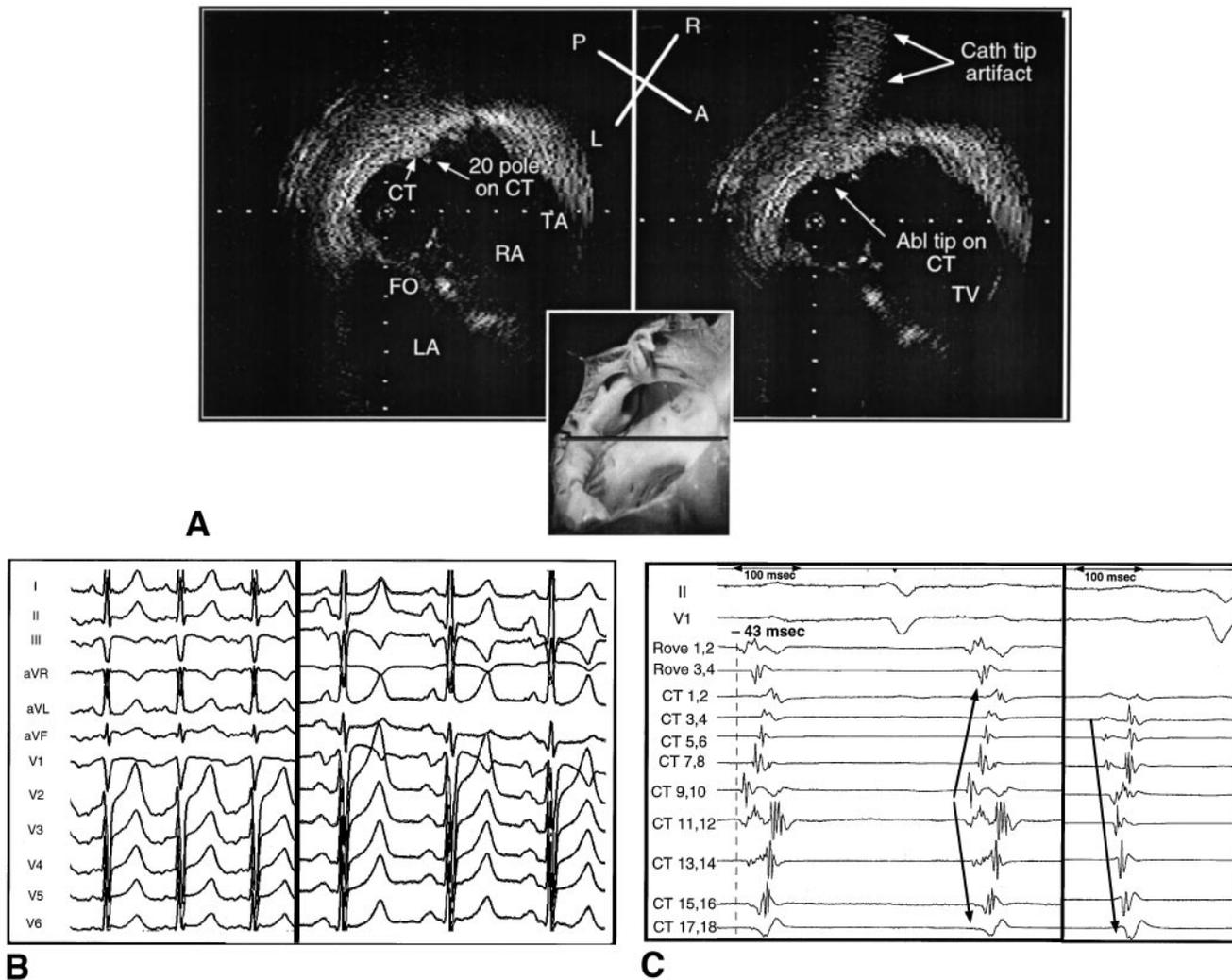
Figure 4. A, ICE view of the mid-CT showing anatomic structures and location of the 20-pole mapping catheter **(left panel),** and with the catheter in place at the site of successful ablation **(right panel). Inset** demonstrates the level of the ICE section. **B,** Twelve-lead ECG showing sinus rhythm **(right panel)** and atrial tachycardia arising from the mid-CT **(left panel)** from the same patient. **C,** Endocardial activation pattern recorded on the 20-pole catheter (CT 1 to 20) during atrial tachycardia arising from the mid-CT **(left panel)** and during sinus rhythm **(right panel).** The roving catheter is located on the mid-CT at the site of successful ablation. Activation is earliest at CT 9,10, where a fractionated, early signal is recorded. The roving catheter at the mid-CT site of successful ablation records a similarly early and fractionated signal. The presence of split components and fractionation elsewhere on the CT during both atrial tachycardia and sinus rhythm suggests extensive cellular uncoupling along the CT in this patient. During sinus rhythm, earliest activation is recorded on the CT catheter at bipole 3,4 and proceeds inferiorly in a high to low sequence. RA = right atrium; other abbreviations as in Figures 1 to 3.

superior CT. Two of four right pulmonary vein tachycardias had an inverted P wave in lead aVL (50%, 95% CI 7% to 93%). Lead V_1 was positive in 4 of 27 (15%, 95% CI 4% to 34%) right atrial tachycardias and 2 of 4 right pulmonary vein tachycardias (50%, 95% CI 7% to 93%).

Endocardial activation mapping. Endocardial activation mapping was facilitated by placement of a 20-pole catheter along the CT by using ICE. Activation times for the various tachycardia locations are shown in Table 2. Several distinct patterns of activation along the CT were identified.

Right atrial tachycardias. For tachycardias located on the high CT, earliest activation was at the superior region of the 20-pole CT mapping catheter (mean -32 ± 19 ms at bipole 1,2, 95% CI -46 to -19), which demonstrated a high to low activation sequence (Fig. 3C) resembling that of sinus rhythm. For tachycardias located on the mid-CT, earliest activation occurred in the midregion of the CT catheter (mean -30 ± 20 ms at bipole 9,10, 95% CI -47 to -12) and the activation sequence proceeded in a V-shaped pattern from this site (Fig. 4C). For tachycardias located on the low CT, earliest activation was at the inferior region of the 20-pole crista mapping catheter (mean -47 ± 8 ms at bipole 19,20), which demonstrated a low to high activation sequence. In 16 of 18 (89%, 95% CI 65% to 99%) tachycardias arising from the CT, an activation time of -25 ms was identified from at least one of

Table 1. P Wave Configuration by Tachycardia Location

Tachycardia Location	ECG Lead					
	I	aVL	V_1	II	III	aVF
High CT						
Positive	8	4	3	9	9	10
Negative	1	4	3	—	—	—
Biph/iso	1	2	4	1	1	—
Mid-CT						
Positive	6	3	1	4	3	4
Negative	—	—	2	—	1	—
Biph/iso	—	3	3	2	2	2
Low CT						
Positive	—	2	—	—	—	—
Negative	—	—	2	2	2	2
Biph/iso	2	—	—	—	—	—
RUPV						
Positive	3	2	3	3	3	3
Negative	—	2	—	—	—	—
Biph/iso	1	—	1	1	1	1
TA						
Positive	3	3	—	—	—	—
Negative	—	—	3	1	2	1
Biph/iso	—	—	—	2	1	2
CS os						
Positive	—	2	—	—	—	—
Negative	—	—	1	2	2	2
Biph/iso	2	—	1	—	—	—

Biph/iso = biphasic/isoelectric; CS = coronary sinus; CT = crista terminalis; ECG = electrocardiographic; RUPV = right upper pulmonary vein; TA = tricuspid annulus.

the bipoles of the 20-pole mapping catheter. In contrast, only one of nine (11%, 95% CI 0% to 48%) tachycardias arising off the CT demonstrated an activation time of −25 ms (p < 0.001).

Left atrial tachycardias. For tachycardias located in the right pulmonary veins, activation along the length of the 20-pole mapping catheter was relatively on time, with absence of a definite sequence, and activation times along the length of the CT were not early in relation to P wave onset (Fig. 5, Table 2).

ICE clearly demonstrated the proximity of the right pulmonary vein orifice to the superior vena cava–right atrial junction and the superior CT at this level (Fig. 6). To assist differenti-
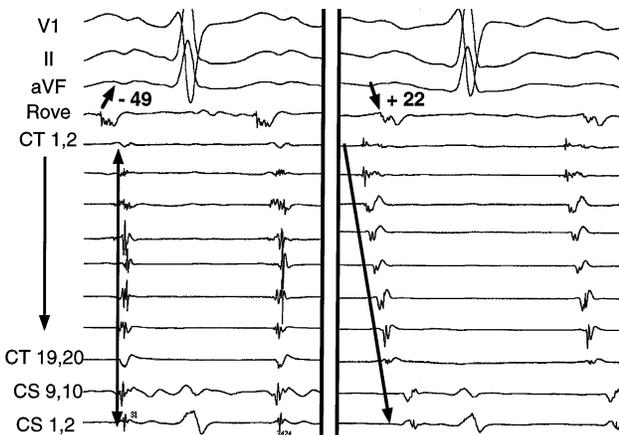

Figure 5. Endocardial activation pattern recorded on the 20-pole catheter (CT 1 to 20) during atrial tachycardia arising from the right upper pulmonary vein **(left panel)** and during sinus rhythm **(right panel).** The roving catheter is located in the right upper pulmonary vein at the site of successful ablation. During tachycardia the activation sequence on the CT catheter is "on time," and the roving catheter shows an early and fractionated signal. During sinus rhythm, the CT catheter activation sequence is now high to low on the CT, and the roving catheter at the same site in the pulmonary vein now records a late signal.

ation of atrial tachycardias located on the high CT from those in the right-sided pulmonary veins, ICE was used to guide subtle rotational mapping in this region. When activation was earliest in the posteroseptal area immediately opposite the right pulmonary vein orifice, this suggested a pulmonary vein tachycardia. When activation was earliest in the anterolateral region on the CT, particularly when fractionated, this was indicative of a high "cristal" tachycardia. For each of the four right pulmonary vein tachycardias, activation was significantly earlier at the posteroseptal right atrium (mean −12 ± 8 ms, 95% CI −20 to −5) than at the superior CT (22 ± 4 ms, 95% CI 19 to 25, p < 0.001) or than any other right atrial site. When this was the earliest site and a fractionated signal was not recorded, a transseptal procedure was performed and mapping was directed to the mouth of the right pulmonary veins. For all nine high cristal tachycardias, activation was significantly earlier on the superior CT (−32 ± 19 ms, 95% CI −46 to −19) than at the posteroseptal region (−15 ± 10 ms, 95% CI −22 to −8, p < 0.001) (Table 2). However, there was no absolute

Table 2. Activation Timing by Tachycardia Location

Mapping Site	High CT	Mid-CT	Low CT	RPV	TA
High CT (bipole 1,2)	*−32 ± 19*	4.8 ± 12.5	18.5 ± 9.2	22 ± 4	14 ± 19
Mid-CT (bipole 9,10)	−9 ± 13	*−30 ± 20*	−17 ± 7	22 ± 5	−15 ± 18
Low CT (bipole 19,20)	19 ± 13	14 ± 10	*−47 ± 8*	24 ± 7	−30 ± 26
High posteroseptal	−15 ± 20	2 ± 27	22 ± 12	*−12 ± 8*	NA
HBE	19 ± 30	30 ± 37	25 ± 14	33 ± 17	58 ± 17
CS os (bipole 9,10)	51 ± 18	46 ± 28	−2 ± 2	48 ± 28	22 ± 33
CS distal (bipole 1,2)	77 ± 30	84 ± 37	53 ± 35	77 ± 24	70 ± 45

HBE = His bundle electrogram; RPV = right pulmonary vein; other abbreviations as in Table 1. Numbers in italics indicate site of earliest activation.
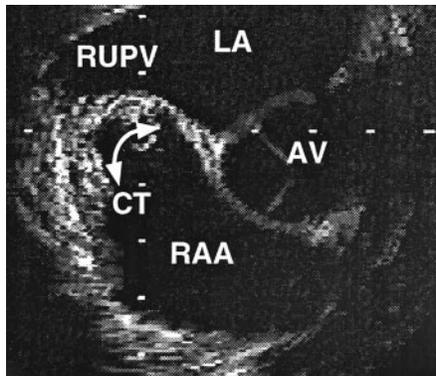
Figure 6. ICE section through the level of the high right atrium showing the superior CT and its relation to the right upper pulmonary vein (RUPV). The **arrow** demonstrates the area of mapping guided by ICE to differentiate between a high cristal tachycardia and one in the right upper pulmonary vein (see text). AV = aortic valve; other abbreviations as in Figure 1.

difference in activation timing at the high posterior septum between high "cristal" tachycardias (-15 ± 10 ms) and right pulmonary vein tachycardias (-12 ± 8 ms, p = 0.6).

Radiofrequency ablation. Radiofrequency ablation was successful in 26 of 27 (96%, 95% CI 81% to 100%) right atrial tachycardias and 3 of 4 (75%, 95% CI 19% to 99%) left atrial tachycardias (overall 29 of 31 tachycardias [94%, 95% CI 79% to 99%]). Ablation was successful in 25 of 27 patients (93%, 95% CI 76% to 99%). The mean number of radiofrequency applications was 5.2 ± 5.7 (median 4, 95% CI 3 to 7). The mean fluoroscopy time was 34 ± 27 min (95% CI 22 to 46).

A fractionated electrogram was recorded at the successful site of ablation in 26 of 29 (90%, 95% CI = 73% to 98%) tachycardias (Fig. 3B and 4B). Before radiofrequency application, exit block from a tachycardia focus was recorded in two patients. In one there was a 2:1 relation and in one a more complex relation demonstrating competition with a second tachycardia focus elsewhere in the right atrium. In one patient, entrance block into a tachycardia focus was observed with the focus demonstrating parasystolic beating.

The mean activation time at the successful ablation site was -47 ± 18 ms (95% CI -54 to -40). Speeding of tachycardia before termination during the radiofrequency application occurred in 22 of 28 (79%, 95% CI 59% to 92%) tachycardias in which the application was performed during tachycardia.

Ablation failed in one patient with three different atrial tachycardia foci in the right atrium. Two of the foci were successfully mapped and ablated (one in the vicinity of the ostium of the coronary sinus and one along the mid-CT). A third focus, which was mapped to the region of the anterior right atrial appendage, could not be successfully ablated. Ablation also failed in one patient with a tachycardia located in the inferior region of the right upper pulmonary vein. An early site was identified and transient success achieved. However, adequate catheter stability and tissue heating could not be achieved.

Follow-up. There were no immediate or long-term complications from the procedure. In the 25 patients with an initially successful ablation, there have been four tachycardia recurrences (16%, 95% CI 5% to 36%). All of these recurrences occurred within 6 weeks (2, 3, 4 and 6 weeks after the procedure). Two patients underwent successful repeat ablation. In a third, symptoms disappeared spontaneously 6 months after ablation and no further medical therapy has been required. One patient is being managed medically. In the remaining 21 patients there have been no recurrences during a mean follow-up period of 9.9 ± 6.3 months (95% CI 6.7 to 13.1).

Discussion

This study demonstrates that right atrial tachycardias occurring in patients without structural heart disease tend to cluster at certain anatomic sites. Approximately two thirds of these tachycardias will be distributed along the long axis of the CT, with an apparent gradation in frequency from superior to inferior. Although other studies (3,4,14,18) have suggested the CT as a common site for right atrial tachycardias, our study is unique in having added direct endocardial visualization and multipolar mapping along this structure. The incidence of right atrial tachycardias occurring along the CT is similar to that in a preliminary report by Shenasa et al. (14).

Consideration of normal atrial anatomy and physiology allows some speculation as to the particular anatomic distribution of atrial tachycardias observed in this study. The CT is an area of marked anisotropy due to poor transverse cell to cell coupling (19). Such anisotropy, by creating a region of slow conduction, favors the development of microreentry. In addition, the normal sinus pacemaker complex is distributed along the long axis of the CT (20). The presence of automatic tissue together with relative cellular uncoupling may be a requirement for abnormal automaticity such that normal atrium is prevented from electrotonically inhibiting abnormal phase 4 depolarization (21,22).

The presence of poor local cell to cell coupling is suggested by the recording of an early and fractionated signal at the site of successful ablation in 93% of successful radiofrequency applications. This incidence rate is consistent with that of our earlier series (1) and other reported experience (14). These fractionated signals may reflect poor cell to cell coupling causing slowed conduction either from a poorly coupled automatic focus or as part of a small reentrant circuit. Further evidence in support of poor local coupling is provided by examples of exit and entrance block from the tachycardia focus. Other investigators (2,3) have not reported a similarly high incidence of fractionated recordings at the site of successful ablation. Our approach was to actively seek a fractionated signal in areas of early activation. In our experience these signals are recorded in a highly localized area, and it is possible that radiofrequency ablation would be successful in immediately adjacent catheter locations without the presence of these signals. In addition, fractionated signals may be recorded at

any site where poor coupling exists. Thus, the sensitivity and specificity of this observation have not been evaluated.

Noncristal right atrial tachycardias. In this study, one third of right atrial tachycardias did not arise from the CT and were distributed widely around the right atrium. As previously described, right atrial tachycardias also occurred in the posteroseptal area near the ostium of the CS (2,3) and within the body and toward the tip of the right atrial appendage (1,3–5,13). For one atrial appendage tachycardia, we were able to demonstrate its origin from an abnormally prominent mass that was identified only with ICE. It is interesting to speculate that this apparent structural abnormality was associated with abnormalities in cellular function or cell to cell coupling, or both, that formed the substrate for the atrial tachycardia. In addition, we observed that three tachycardias occurred on the tricuspid annulus away from the septum, a location that to our knowledge has not been previously described.

Use of intracardiac echocardiography to guide mapping. *Cristal tachycardias.* The use of ICE during the ablation procedure helps to emphasize the unique and complex anatomy of the right atrium and demonstrates the importance of linking mapping with known endocardial anatomy (10,11). Accurate placement of a multipolar catheter along the CT provided a road map to facilitate mapping. For those tachycardias located on the CT, the multipolar catheter provided a reliable guide to the precise tachycardia area. In view of the previously described variability in anatomic course of the CT (23), ICE was necessary for accurate positioning of this mapping catheter and guiding precise mapping along this structure with the rove catheter. For those tachycardias located off the CT, activation on the multipolar catheter was relatively late and lacked dispersion of activation times. This clearly indicated that sites away from the CT required mapping.

High cristal versus right upper pulmonary vein tachycardias. Although we aimed to characterize the anatomic distribution of right atrial tachycardia foci, four patients with left atrial tachycardias located in the right upper pulmonary veins were also included in the study. This is because the P wave configuration of tachycardias in this location demonstrates considerable overlap with that of tachycardias in the high right atrium on the CT. This is perhaps not surprising when considering the proximity of these two regions and that the right upper pulmonary vein orifice may be rightward of the superior medial CT. Use of ICE in this study clearly demonstrated this close anatomic relation and facilitated careful and subtle mapping to determine whether a tachycardia was high cristal or in the right upper pulmonary vein. This is of importance when making a decision as to whether it is necessary to proceed with a transeptal puncture.

Limitations. The aim of this study was to define the anatomic distribution of focal atrial tachycardias in the right atrium by using ICE and to describe a technique for performing electrophysiologic mapping directed at endocardial landmarks. Although it would appear logical that ability to link endocardial anatomy to electrophysiologic events would facilitate mapping and ablation of atrial tachycardias, we have not

compared the combined use of fluoroscopy and ICE with fluoroscopy alone.

The 10-MHz imaging catheter used in the current study does not permit adequate imaging of left atrial structures other than the entrance of the right pulmonary veins. We have therefore not attempted to characterize the anatomic location of left atrial tachycardias other than those originating in the right pulmonary veins.

Conclusions. This study demonstrates that approximately two thirds of focal right atrial tachycardias occurring in the absence of structural heart disease will arise from along the CT. Placement of a multipolar mapping catheter along the CT under ICE guidance provided a clear guide to the tachycardia origin. Recognition of this common distribution may facilitate mapping and ablation of these tachycardias. Further study will be required to determine whether use of ICE leads to an increased success rate or a reduction in fluoroscopy or procedure time.

References

1. Lesh MD, Van Hare GF, Epstein LM, et al. Radiofrequency catheter ablation of atrial arrhythmias—results and mechanisms. Circulation 1994; 89:1074–89.
2. Tracy CM, Swartz JF, Fletcher RD, et al. Radiofrequency catheter ablation of ectopic atrial tachycardia using paced activation sequence mapping. J Am Coll Cardiol 1993;21:910–7.
3. Kay GN, Chong F, Epstein AE, Dailey SM, Plumb VJ. Radiofrequency ablation for treatment of primary atrial tachycardias. J Am Coll Cardiol 1993;21:901–9.
4. Walsh EP, Saul JP, Hulse JE, et al. Transcatheter ablation of ectopic atrial tachycardia in young patients using radiofrequency current. Circulation 1992;86:1138–46.
5. Poty H, Saoudi N, Haissaguerre M, Daou A, Clementy J, Letac B. Radiofrequency catheter ablation of atrial tachycardias. Am Heart J 1996; 131:481–9.
6. Pappone C, Stabile G, DeSimone A, et al. Role of catheter-induced mechanical trauma in localization of target sites of radiofrequency ablation in automatic atrial tachycardia. J Am Coll Cardiol 1996;27:1090–7.
7. Tang CW, Scheinman MM, Van Hare GF, et al. P wave morphology during automatic atrial tachycardia in man. J Am Coll Cardiol 1995;26:1315–24.
8. Chu E, Fitzpatrick AP, Chin MC, Sudhir K, Yock PG, Lesh MD. Radiofrequency catheter ablation guided by intracardiac echocardiography. Circulation 1994;89:1301–5.
9. Chu E, Kalman JM, Kwasman MA, et al. Intracardiac echocardiography during radiofrequency catheter ablation of cardiac arrhythmias in man. J Am Coll Cardiol 1994;24:1351–7.
10. Olgin JE, Kalman JM, Fitzpatrick AP, Lesh MD. The role of right atrial endocardial structures as barriers to conduction during human type 1 atrial flutter: activation and entrainment mapping guided by intracardiac echocardiography. Circulation 1995;92:1839–48.
11. Kalman JM, Lee RJ, Fisher WG, et al. Radiofrequency catheter modification of sinus pacemaker function guided by intracardiac echocardiography. Circulation 1995;93:3070–81.
12. Lee RJ, Kalman JM, Fitzpatrick AP, et al. Radiofrequency catheter modification of the sinus node for inappropriate sinus tachycardia. Circulation 1995;93:2919–28.
13. Chen SA, Chiang CE, Yang CJ, et al. Sustained atrial tachycardia in adult patients: electrophysiological characteristics, pharmacological response, pos-

sible mechanisms and effects of radiofrequency ablation. Circulation 1994;
90:1262–78.

14. Shenasa H, Merrill JJ, Hamer ME, Wharton JM. Distribution of ectopic atrial tachycardias along the crista terminalis: an atrial ring of fire [abstract]? Circulation 1993;88 Suppl I:I-29.

15. Gillette P, Garson AJ. Electrophysiologic and pharmacologic characteristics of automatic ectopic atrial tachycardia. Circulation 1977;15:1345–54.

16. Olshansky B, Okumura K, Hess PG, Waldo AL. Demonstration of an area of slow conduction in human atrial flutter. J Am Coll Cardiol 1990;16:1639–48.

17. Stevenson WG, Sager PT, Friedman PL. Entrainment techniques for mapping atrial and ventricular tachycardias. J Cardiovasc Electrophysiol 1995;6:201–16.

18. Sanders WE Jr, Sorrentino RA, Greenfield RA, Shenasa H, Hamer ME, Wharton JM. Catheter ablation of sinus node reentrant tachycardia. J Am Coll Cardiol 1994;23:926–34.

19. Saffitz JE, Kanter HL, Green KG, Tolley TK, Beyer EC. Tissue-specific determinants of anisotropic conduction velocity in canine atrial and ventricular myocardium. Circ Res 1994;74:1065–70.

20. Boineau JP, Canavan TE, Schuessler RB, Cain ME, Corr PB, Cox JL. Demonstration of a widely distributed atrial pacemaker complex in the human heart. Circulation 1988;77:1221–37.

21. de Bakker JM, Hauer RN, Bakker PF, Becker AE, Janse MJ, Robles de Medina EO. Abnormal automaticity as mechanism of atrial tachycardia in the human heart—electrophysiologic and histologic correlation: a case report. J Cardiovasc Electrophysiol 1994;5:335–44.

22. Joyner R, Van Capelle F. Propagation through electrically coupled cells: how a small SA node drives a large atrium. Biophys J 1996;50:1157–64.

23. Weiss C, Hatala R, Carpinteiro L, Halata Z. Topographic anatomy and in vitro fluoroscopic imaging of the crista terminalis: an attempt to more precisely localize the origin of ectopic atrial tachycardia [abstract]. Circulation 1994;90 Suppl I:I-595.